Journal of Solid Mechanics Vol. 16, No. 1 (2024) pp. 1-13
DOI: 10.60664/jsm.2024.1129238

Research Paper

# Numerical Implementation of A Nonlocal Damage Model For A Stress Regime-Dependent Creep Constitutive Model

B. Hajivand Dastgerdi *, M. Baghani

*School of Mechanical Engineering, College of Engineering, University of Tehran, Tehran, Iran*

Received 03 March 2023; Received in revised form 26 September 2023; Accepted 25 September 2023

**ABSTRACT**

Several components of aeronautical motors and power plant stations are subjected to high temperatures, leading to creep deformation. It's common practice to predict crack development in such components by using Continuum Damage Mechanics (CDM). Nevertheless, mesh dependency is a well-known issue in the classical CDM approach. The mesh sensitivity problem can be solved by using a nonlocal continuum approach. In the present study, in order to improve the numerical efficiency, a stress regime dependent creep model has been extended to a nonlocal model using a nonlocal theory from the literature. The nonlocal creep model was applied to a commercial finite element code, such as ABAQUS, with the help of user-defined routines (CREEP+USDFLD) to predict the load point displacement (LPD) and creep crack growth (CCG) for a compact tension (CT) specimen made of high creep strength 1CrMoV steel. A comparison between the results of the new nonlocal model and experimental data was made for verification. The mesh dependency of the new nonlocal model was investigated. The results indicate that the proposed nonlocal creep model demonstrates good mesh objectivity that was not feasible when considering the traditional local creep model.

**Keywords:** Creep constitutive model; Stress regime-dependent creep behavior; Finite element; Continuum damage mechanics; Nonlocal damage; 1CrMoV Alloy.

## 1 INTRODUCTION

THE components of aeronautical motors and power plant stations usually encounter fluctuating loads at high temperatures, leading to creep deformation. Due to the combined effect of mechanical and thermal loads, the

*Corresponding author. Tel.: +98 9387693358.
*E-mail address: behzad.hajivand@ut.ac.ir*
.

degradation rate of the material properties increases in this situation. A combination of creep and fatigue occurs simultaneously when cyclic loads are applied at high temperatures, commonly described as creep fatigue interaction (CFI) [1]. Microscopic defects such as micro-cracks/voids can be formed in these components upon loading. Therefore, to guarantee component safety, the effect of these adverse events on components should be investigated. Structural analysis and lifetime evaluation of these elements require analysis of creep crack growth (CCG) simulations [2].

Several computational approaches have been developed to determine the life of these components. One of these approaches that has attracted many researchers is Continuum Damage Mechanics (CDM). It's common practice to predict crack development in such components by using CDM. Numerous creep constitutive models have been established over the past years, and a number of them have been reviewed by Holdsworth et al. [3]. A power law equation was proposed by Norton [4] to describe the behavior of secondary creep deformation. Kachanov [5] used this model to describe the creep deformation in a brittle material by introducing the concept of effective stress. Rabotnov [6] modified this model, known as the Kachanov-Rabotnov model, by introducing a damage variable that depends on the effective stress. However, this model was strongly mesh-dependent for the prediction of CCG. Murakami et al. [7, 8, 9] investigated the effectiveness of the local and nonlocal formulations on the prediction of the CCG simulations. Hyde et al. [10-15] used Liu-Murakami's creep damage model to investigate the CCG by the finite element method. Using a general single formulation to capture the behavior of materials in all stress regimes (such as single-regime or secondary-regime creep) proposed in many creep deformation models [4, 16, 17]. Nevertheless, a creep deformation model that can simultaneously describe three stages of creep deformation (primary, secondary, and tertiary) is less frequently discussed in the literature. Therefore, Hosseini et al. [2] proposed their more physically acceptable stress regime-dependent creep model.

To more accurately depict the physics during creep fatigue behavior, Xiao [18] presented a new creep and fatigue damage model. Based on a number of creep fatigue damage curves, Skelton and Gandy [19] constructed a nonlinear coupled CFI model. Additionally, Zhao [20], Xu [21], and Tang [22] used Skelton and Gandy's damage model to conduct creep fatigue crack growth simulations. To analyze the creep fatigue failure, Fan [23] developed a fatigue damage model. Huang [24] introduced a creep-fatigue model to predict creep-fatigue life efficiently. Liu [25] developed a nonlinear creep fatigue damage model to perform creep fatigue crack growth simulations.

All the previously mentioned simulations were studied using the local approach and are classified as classical local continuum theories. In classical continuum mechanics, each point of material only interacts with its nearest neighbor. The inability of the classical continuum theory to describe strain softening and localization due to the lack of information on the size of the localization zone is one of its major disadvantages [26].

It has been reported in the literature that applying the finite element method to local creep damage in order to predict the CCG leads to spurious mesh dependency, making the results unreliable and unrealistic [8]. Early investigations [27-31] verified that the local models are mesh-dependent, especially in stress concentration regions. Consequently, nonlocal internal formulations and gradient formulations were used to reduce or even eliminate this drawback of numerical results. Over the past years, Numerous sophisticated nonlocal methods [32-39] have been developed to resolve this issue and provide realistic and more acceptable results.

The mesh sensitivity problem can be solved by using a nonlocal continuum in which the physical state of a specific point depends not only on its own state but also on a specific neighborhood of that point. Mao and Shen [40] presented their nonlocal damage model, which is easily used in finite element codes such as ABAQUS. In this method, the nonlocal damage variable is averaged using an interpolation function on the surrounding elements, within the range of the characteristic length. To investigate the reliability, the proposed model in conjunction with the constitutive model of an aluminum alloy was implemented in ABAQUS. In the recent past, CDM has been combined with the extended finite element method (XFEM) to predict CCG using coarser meshes [41-47]. However, there are many creep constitutive models in the literature that do not combine with nonlocal theories.

The main objective of the present study is to reduce the mesh sensitivity of a stress regime dependent creep model using a nonlocal approach from the literature. This is accomplished by incorporating a nonlocal approach given by Mao and Shen [40] into the stress regime dependent creep model proposed by Hosseini et al. [2] which was not considered in the literature. The new nonlocal creep model, with the help of user-defined routines (CREEP+USDFLD), was implemented in the ABAQUS program to predict the load point displacement (LPD) and creep crack growth (CCG) of a compact tension (CT) specimen made of the high creep strength 1CrMoV steel. To check the mesh dependency of the new nonlocal model, a comparison between the results of the new proposed model and the traditional local model was conducted.

## 2 FORMOLATION OF THE PROBLEM

Hosseini et al. [2] proposed a more physically acceptable stress regime-dependent creep model that simultaneously describes three stages of creep deformation (primary, secondary, and tertiary). This can be achieved simply by adding the primary, secondary, and third phases of strains [48, 49].

$$\varepsilon_{Total} = \varepsilon_{Primary} + \varepsilon_{Secondary} + \varepsilon_{Tertiary} \tag{1}$$

The creep model used in the present study, which was proposed by Hosseini et al. [2], has the ability to provide appropriate solutions for predicting the creep strain by considering the stress regime dependency. The final uniaxial and multiaxial forms of the creep strain rate model with consideration of stress regime dependency are expressed in the framework of local continuum damage theory as below:

$$\dot{\varepsilon} = A_1 sinh\left[B_1 \frac{(1-H)}{(1-\varphi)(1-\omega_{loc})}\sigma\right] + B_2\left[\frac{(1-H)}{(1-\omega_{loc})}\sigma\right]^n \tag{2}$$

$$\dot{H} = \frac{C_1}{\sigma^\alpha}\left[1-\frac{H}{H^*}\right]\dot{\varepsilon} \tag{3}$$

$$\dot{\varphi} = \frac{C_2}{3}(1-\varphi)^4 \tag{4}$$

$$\dot{\omega}_{loc} = N(C_3\sigma^{v_1} + C_4\sigma^{v_2}\mathcal{H}^{\gamma_2})\frac{(1-e^{-q_2})}{q_2}e^{q_2\omega_{loc}} \tag{5}$$

And

$$\dot{\varepsilon}_{ij} = \frac{3S_{ij}}{2\sigma_e}\left\{A_1 \sinh\left[B_1 \frac{(1-H)}{(1-\varphi)(1-\omega_{loc})}\sigma_e\right] + B_2\left[\frac{(1-H)}{(1-\omega_{loc})}\sigma_e\right]^n\right\} \tag{6}$$

$$\dot{H} = \frac{C_1}{\sigma_e^\alpha}\left[1-\frac{H}{H^*}\right]\dot{\varepsilon}_e \tag{7}$$

$$\dot{\varphi} = \frac{C_2}{3}(1-\varphi)^4 \tag{8}$$

$$\dot{\omega}_{loc} = N\left(C_3\sigma_e^{v_1} + C_4\sigma_e^{v_2}\mathcal{H}^{\gamma_2}\right)\frac{(1-e^{-q_2})}{q_2}e^{q_2\omega_{loc}} \tag{9}$$

Where, $\sigma_e$ is the Mises equivalent stress, $\dot{\varepsilon}_e$ is strain rate value, $S_{ij}$ is the deviatoric stress tensor and $\dot{\varepsilon}_{ij}$ represents the creep strain rate tensor. $\omega_{loc}$ denotes the local damage variable and is active only under tensile stresses. So, if $\sigma_1 > 0$ then $N = 1$ otherwise $N = 0$.

In the following, the nonlocal damage method proposed by Mao and Shen [40] is applied to the aforementioned local creep model. In order to calculate the nonlocal damage increment at a point $x$ a weight function is used to average the local damage increment in a certain domain, $\Omega$, which is determined by the characteristic length.

$$d\omega_{nonloc}(x) = \frac{1}{V}\int_\Omega d\omega_{loc}(s)\phi(s-x)d\Omega(s) = \frac{1}{\int_\Omega \phi(s-x)d\Omega}\int_\Omega d\omega_{loc}(s)\phi(s-x)d\Omega(s) \tag{10}$$

Where $\omega_{loc}$ is local damage variable and $\phi(s)$ is the weight function as follows.

$$\phi(s) = exp\left(-\frac{3(\xi^2+\eta^2+\zeta^2)}{2l^2}\right) \tag{11}$$

Where $\xi$, $\eta$ and $\zeta$ represent the first, second, and third coordinate of the vector $s$. $l$ is the characteristic length that specifies the domain to which the nonlocal calculation should be applied. Then, Taylor's expansion of the local damage increment, $d\omega_{loc}$, about the point $x$ given below:

$$d\omega_{loc}(s) = d\omega_{loc}(x) + \nabla d\omega_{loc}(x)\cdot(s-x) + \frac{1}{2!}\nabla^2 d\omega_{loc}(x)\cdot(s-x)\cdot(s-x) + \frac{1}{3!}\nabla\nabla^2 d\omega \cdot(s-x)\cdot(s-x)\cdot(s-x) + + \frac{1}{4!}\nabla^2\nabla^2 d\omega_{loc}(x)\cdot(s-x)\cdot(s-x)\cdot(s-x) + \cdots \tag{12}$$

By replacing the equations (12) and (11) into the nonlocal damage increment equation (equation (10)) and calculating the integration, $d\omega_{nonloc}$ is obtained as follows:

$$d\omega_{nonloc}(x) = d\omega_{loc}(x) + \frac{1}{2} l^2 \nabla^2 d\omega_{loc}(x) \tag{13}$$

The second order gradient term is achieved by comparing the above equation with the nonlocal damage increment equation (equation (10)):

$$\nabla^2 d\omega_{loc}(x) = \frac{2\left(\int_\Omega \omega_{loc}(s)\phi(s-x)d\Omega(s) - d\omega_{loc}(x)\int_\Omega \phi(s-x)d\Omega(s)\right)}{l^2\int_\Omega \phi(s-x)d\Omega(s)} \tag{14}$$

It is crystal clear that when $\nabla^2 d\omega_{loc}(x) = 0$ the nonlocal model turns to its corresponding local model.

## 3 METHOD OF SOLUTION

The nonlocal creep model was applied to the FEM program ABAQUS (version 6.17) with the help of user-defined routines (CREEP+USDFLD) to evaluate the load point displacement (LPD) and creep crack growth (CCG) for a compact tension (CT) specimen made of the high creep strength 1CrMoV steel at 550 $^\circ C$. Due to the wide range of stresses (from high to low) at the crack tip of the CT specimen, inspecting creep deformation in that can be a reliable test for this model. For calculating the nonlocal damage variable, the local damage value needs to be computed first. The algorithm of the local procedure of the ABAQUS code is shown in Fig. 1. To investigate the reliability of the nonlocal creep model, the load point displacement (LPD) and crack growth (CCG) for different mesh sizes at the crack tip (0.06mm, 0.08mm, 0.1 mm, 0.12mm, 0.3mm, and 0.5mm) are reported. A comparison between the local and nonlocal models, at the load level of 18 KN, was conducted.

The Elastic modulus and Poisson ratio are 150 GPa and 0.3 respectively. According to the value of the damage parameter, the elasticity modulus has been updated $E = E_0/(1-\omega)$. Rate independent plasticity was not taken into account in the calculations. The chosen CETOL parameter in the presented FECDM calculations was $10^{-4}$. The desired geometry was created as a conventional ABAQUS mesh using 21,770 quadratic hexahedral elements (element size of 0.1mm at the crack tip). Fig. 2 shows the shape of the specimen and its dimensions.

### *3.1 Nonlocal Damage Consideration*

To calculate the nonlocal damage value of the current Gauss integration point (IP), we require the information of the current IP from the ABAQUS main program as well as the information of other IPs placed within the domain specified by the characteristic length.

To achieve this purpose, a common block is introduced to store the coordinates of the Gaussian points and the damage variables associated with them. The common block, defined as ENCD, is a three-dimensional array. The first dimension identifies the element, the second dimension identifies the IP, and the third dimension contains the coordinates of the IP and the damage variable value associated with it. They are updated after the associated IP has been processed at the end of each time step. Once the local values are obtained, the nonlocal damage gradient is calculated as follows:

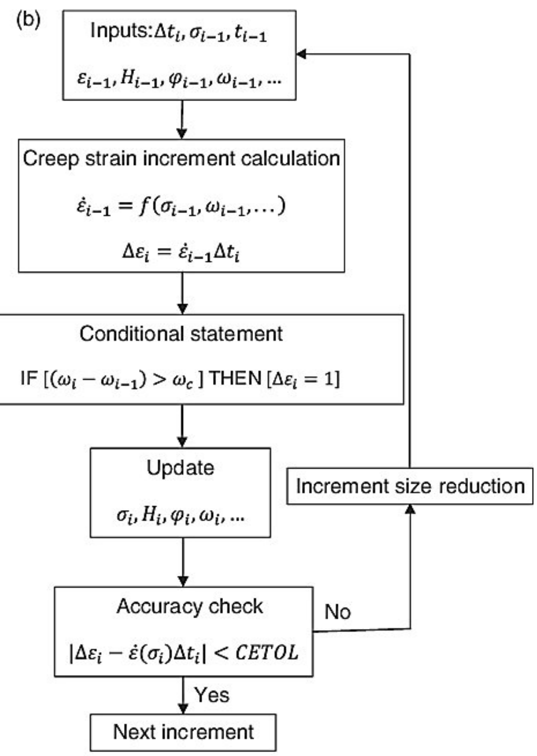


**Fig. 1**
The algorithm of local creep strain model used by ABAQUS code [2].

$$d\omega_i = \sum_{j=1}^{GP} \phi_j \Delta\omega_j \Big/ \sum_{j=1}^{GP} \phi_j \tag{15}$$

Where $i$ denotes the current calculated IP, $j$ is the IP in the domain of characteristic length, and GP refers to the total number of IP in the domain. For more information, refer to [40].

## 4 RESULTS AND DISCUSSION

To validate the nonlocal creep model and check the mesh sensitivity, a compact tension (CT) specimen is modelled in the ABAQUS program. By cause of symmetry, a quarter model with quadratic hexahedral elements was used. Due to the stress concentration near the crack tip, a fine mesh is used in this area. Constant load creep crack incubation (CCI) tests at 550 $^\circ C$ for the CT specimen, which were reported by Holdsworth and Mazza [50] are used to verify the results.

### *4.1 The Effect of characteristic length*

The Characteristic Length is an important parameter in the nonlocal model, as it determines an area close to the currently calculated material point. Obviously, the nonlocal model turns to the traditional local model when the Characteristic Length is equal to zero. As mentioned earlier, the characteristic length determines the amount of material elements to be considered in the nonlocal calculations. To determine the optimum value of the characteristic length for the proposed nonlocal model, a comparison between the experimental LPD records at the crack tip and the FE simulation was made. A finite element simulation at a constant load (18 KN) for different characteristic lengths (from 0 to 3 mm) was performed. Fig. 3 indicates that the optimum size of Characteristic Length for the nonlocal model could be 1.5 mm.

As illustrated in Fig. 3, it would indeed be possible to achieve equally accurate approximations with a higher characteristic length. However, since the greater characteristic length requires more integration points, it takes longer to do calculations and computational efficiency would be reduced. Therefore, the characteristic length is considered to be 1.5 mm in the present work.

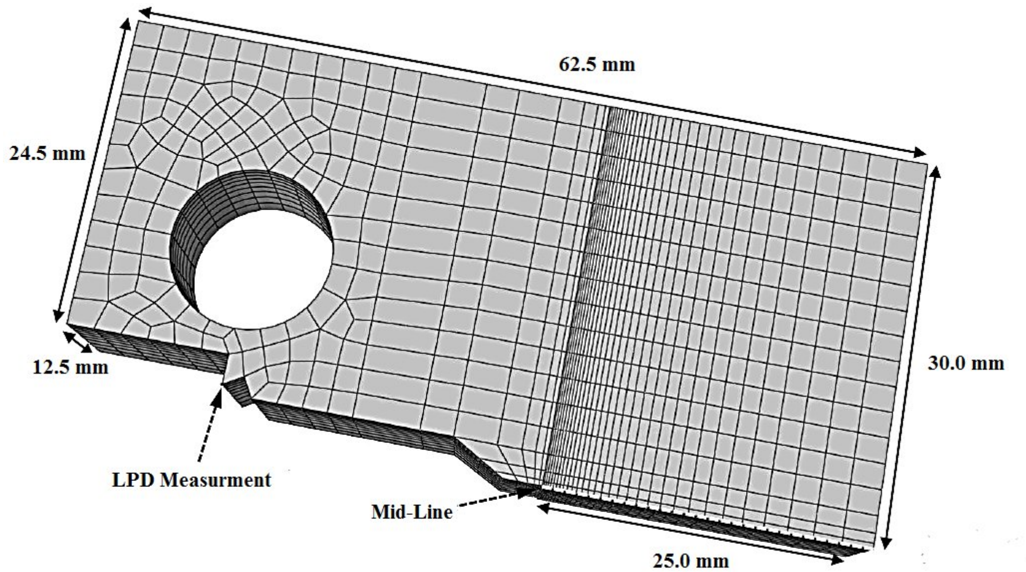


**Fig. 2**
CT specimen with its dimensions.

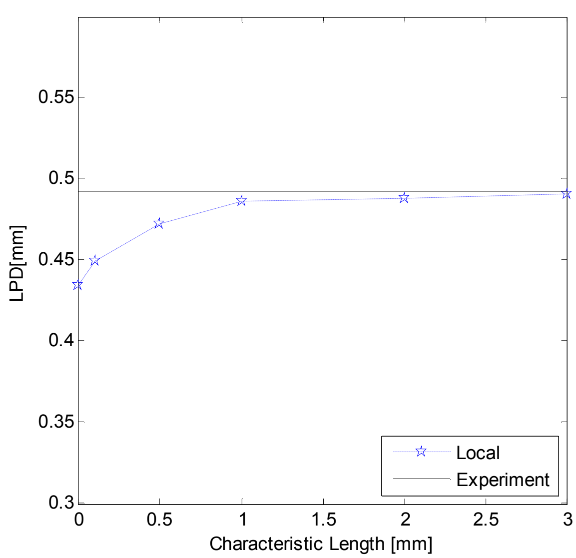


**Fig. 3**
characteristic length verses LPD for constant load 18KN.

### *4.2 Comparison between local and nonlocal results*

The crack development pattern for the local and nonlocal models, with a mesh size of 0.5mm at the crack tip, is compared in Fig. 4. Both local and nonlocal models predicted a plane strain pattern for crack development, which demonstrates an acceptable agreement with experimental results. Although the finite width of the damage zone of the nonlocal model is greater than that of the local model. It is readily apparent that the damage variable in the local creep model is localized over a narrow region in the vicinity of the crack tip.

**Table 1**
Creep constitutive model parameters for 1CrMoV steel at 550

| Parameter Values | $A_1$ | $B_1$ | $B_2$ | n | $C_1$ | $\alpha$ | $H^*$ |
|---|---|---|---|---|---|---|---|
| | $8.2\times10^{-13}$ | 0.12 | $2.2\times10^{-13}$ | 3.00 | $1.2\times10^{-2}$ | $-2$ | 0.54 |
| Parameter Values | $C_2$ | $C_3$ | $\nu_1$ | $C_4$ | $\nu_2$ | $\gamma_2$ | $q_2$ |
| | 0.00 | $2.8\times10^{-47}$ | 17.50 | $2.8\times10^{-14}$ | 3.87 | $0.74\times\nu_2$ | 13.00 |

Fig. 5 represents the predicted LPD versus time for six different element sizes at the crack tip. The central processing unit (CPU) of the notebook is an Intel i5-1135G7 (memory 16GB), and four cores are used for calculation. The running time is different for each mesh size, and it changes from 10 to 30 minutes.

As observed from Fig. 5a, the local model has a serious mesh dependency and also shows that, with the increase in the size of the crack-tip elements, the responses are far from acceptable values. The simulations are performed for the nonlocal model in the same situation. It can be observed from Fig. 4b that objective mesh results are obtained by adopting the nonlocal approach.

**Table 2**
Comparison of local and nonlocal model mesh sensitivity

| Mesh size at crack tip (mm) | End point of the LPD graph for load level of 18 kN | | | | |
|---|---|---|---|---|---|
| | Local Model | | Nonlocal model | | Experiment |
| | Prediction (mm) | Error | Prediction (mm) | Error | |
| 0.06 | 0.4794 | 2.64% | 0.4915 | 0.18% | 0.4924 |
| 0.08 | 0.4738 | 3.78% | 0.4911 | 0.26% | |
| 0.10 | 0.4652 | 5.52% | 0.4910 | 0.28% | |
| 0.12 | 0.4596 | 6.66% | 0.4909 | 0.30% | |
| 0.30 | 0.4308 | 12.5% | 0.4866 | 1.18% | |
| 0.50 | 0.4047 | 17.81% | 0.4863 | 1.23% | |

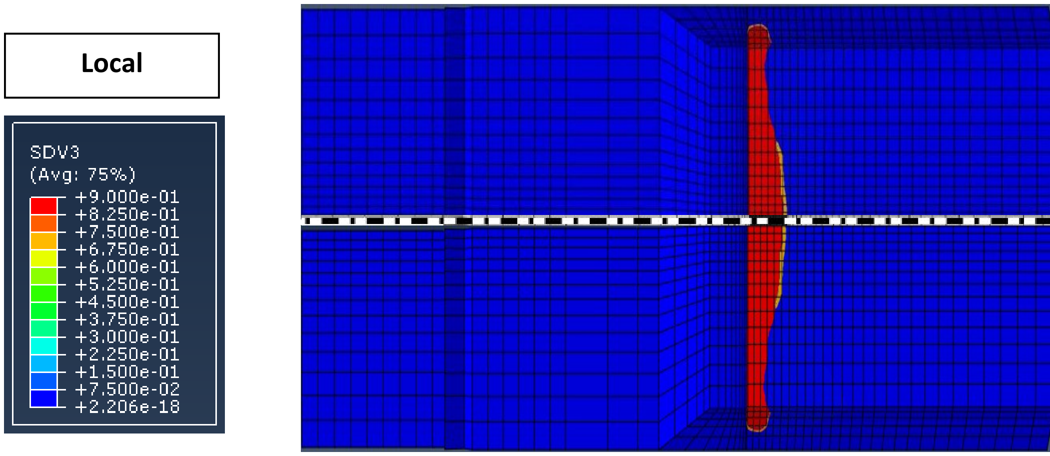


**Fig. 4a**

crack development pattern of the local creep deformation model for the compact tension (CT) specimen at load level 18kN. (SDV3 represent the damage state variable).

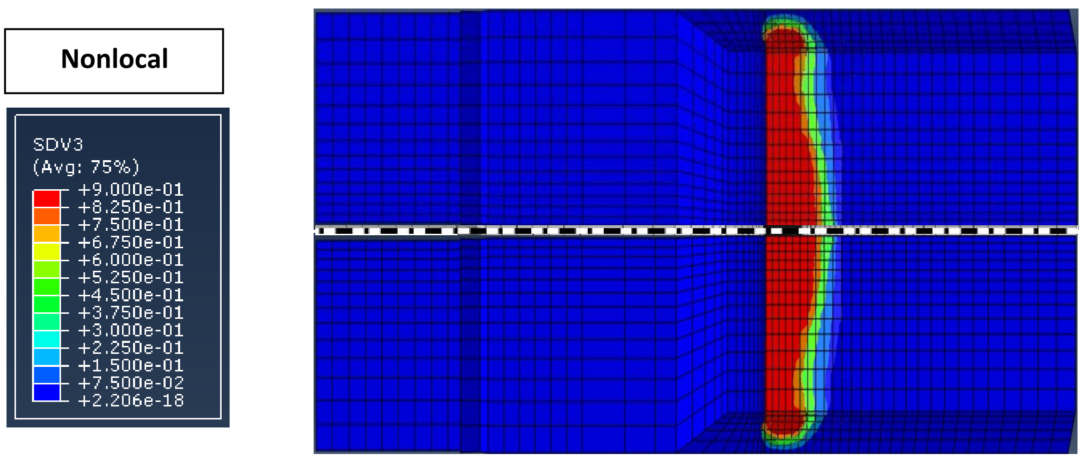


**Fig. 4b**

crack development pattern of the nonlocal creep deformation model for the compact tension (CT) specimen at load level 18kN. (SDV3 represent the damage state variable).

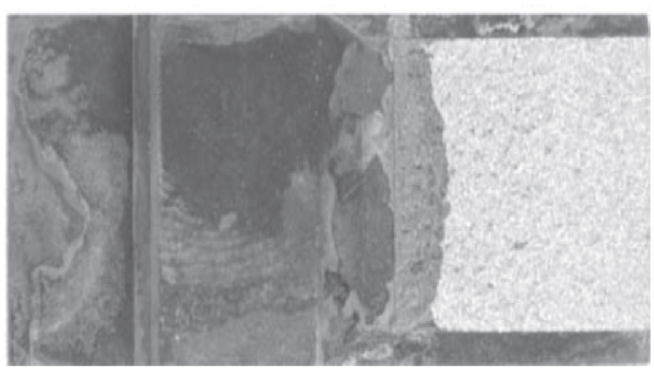

**Fig. 4c**

Experimental observation of crack development pattern for the compact tension (CT) at load level 18kN. For more information, related to experimental data see [50].

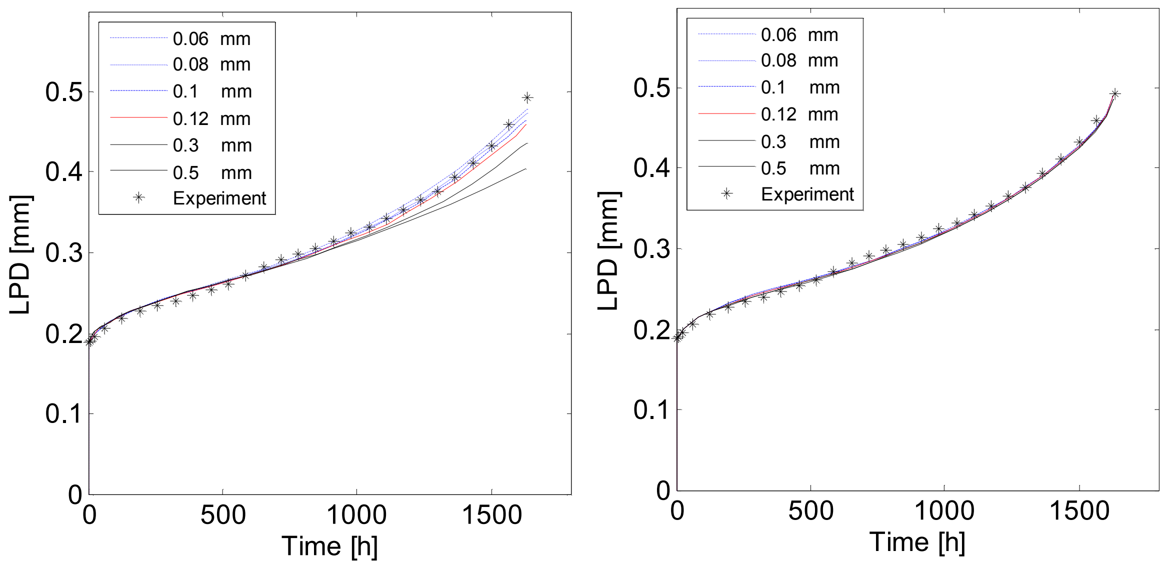


**LOCAL (a)** **NONLOCAL (b)**

**Fig. 5**
Mesh sensitivity of the local and nonlocal model for load level of 18kN (six different sizes of element at the crack tip).

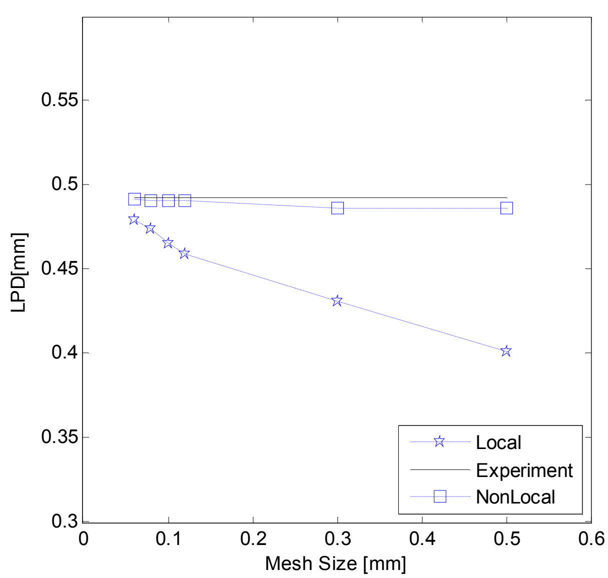


**Fig. 6**
The End point of the LPD graph versus mesh size for the local and nonlocal model.

The maximum discrepancy between the predicted results and experimental data occurred at the end point of the LPD graph (Fig. 5). Therefore, this point, presented in Table 1, is used for a numerical comparison between the local and nonlocal models. The LPD of this point versus mesh size has been plotted in Fig. 6. As seen, when a coarse mesh is employed, the local model shows a maximum error of 17.81% in its prediction. On the contrary, with the assumed 1.5 mm characteristic length for the nonlocal model, this model shows good mesh objectivity, and the errors fall within acceptable values, which demonstrate the accuracy of the nonlocal model.

## 5 CONCLUSIONS

Nonlocal treatment was applied to the local creep model, and these main results were obtained:

- Both the local and nonlocal models predicted a plane strain pattern for crack development, which demonstrates an acceptable agreement with experimental results.
- The finite width of the damage zone in the nonlocal model is greater than the local model in the same loading situation. In other words, the damage variable in the local creep model is localized over a narrow region in the vicinity of the crack tip.
- When a coarse mesh is used (a mesh size of 0.5mm at the crack tip), the local model shows a maximum error of 17.81% in its prediction. On the contrary, with the assumed 1.5 mm characteristic length for the nonlocal model, this model shows good mesh objectivity, and the errors are acceptable values, which demonstrate the accuracy of the nonlocal model.

## 6 NOMENCLATURE

| | |
|---|---|
| $A_1$ | constant values in creep constitutive models |
| $B_1$ , $B_2$ | constant values in creep constitutive models |
| $C_1, C_2, C_3, C_4$ | constant values in creep constitutive models |
| $H, H^*$ | state variable representing primary creep, saturated value for $H$ |
| $\mathcal{H}$ | stress multiaxiality factor, $\sigma_1/\sigma_e$ |
| $n$ | secondary creep stress exponent in low-stress regime |
| $N$ | constant value in creep damage equation |
| $q_2$ | constant value in creep damage equation |
| $S_{ij}$ | deviatoric stress tensor components |
| $\alpha$ | parameter defining the dependency of primary creep strain on stress |
| $\gamma_2$ | stress multiaxiality exponents in creep damage equation |
| $\varepsilon, \dot{\varepsilon}$ | creep strain, creep strain rate |
| $\dot{\varepsilon}_e$ | Von Mises equivalent creep strain rate |
| $\dot{\varepsilon}_{ij}$ | creep strain rate tensor components |
| $\nu_1, \nu_2$ | stress exponents in creep damage equation |
| $\sigma$ | stress |
| $\sigma_1$ | maximum principal stress |

| | |
|---|---|
| $\sigma_e$ | Von Mises equivalent stress |
| $\varphi$ | state variable representing interparticle distance |
| $\omega$ | state variable representing creep damage |
| $\Omega$ | A domain, where the nonlocal treatment is applied. |
| $\phi$ | weight function |
| $l$ | characteristic length |
| $\nabla, \nabla^2$ | the first and second order gradient operator |

## REFERENCES


[1] V.B. Pandey, I.V. Singh, B.K. Mishra, A new creep-fatigue interaction damage model and CDM-XFEM framework for creep-fatigue crack growth simulations, *Theoretical and Applied Fracture Mechanics*, Volume 124, **2023**, 103740, ISSN 0167-844,

[2] Hosseini E, Holdsworth SR and Mazza E, Stress regime-dependent creep constitutive model considerations in finite element continuum damage mechanics. *International Journal of Damage Mechanics*, **2013**; 22(8): 1186–1205.

[3] Holdsworth SR, Abe F, Kern TU and Viswanathan R (eds), Constitutive equations for creep curves and predicting service life. Creep-resistant Steels. Cambridge, England: *Woodhead Publishing and CRC Press*, **2008**; pp. 403–420.

[4] Norton FH, The Creep of Steel at High Temperature. New York: McGraw-Hill, **1929**.

[5] Kachanov, L. M., Time of rupture process under varying strain gradients (in Russian), *Izvestia Akademii Nauk*, USSR, **1958**; No. 8, pp: 26-31.

[6] Rabotnov YN, Creep Problems in Structural Members. Amsterdam: North-Holland, **1969**.

[7] Murakami S, Kawai M and Rong H Finite element analysis of creep crack growth by a local approach. *International Journal of Mechanical Sciences*, **1988**; 30(7): 491–502.

[8] Murakami S and Liu Y, Mesh-dependence in local approach to creep fracture. *International Journal of Damage Mechanics*, **1995**; 4(3): 230–250.

[9] Murakami S, Liu Y and Mizuno M, Computational methods for creep fracture analysis by damage mechanics. *Computer Methods in Applied Mechanics and Engineering*, **2000**; 183(1): 15–33.

[10] Hyde CJ, Hyde TH, Sun W, et al., Damage mechanics-based predictions of creep crack growth in 316 stainless steel *Engineering Fracture Mechanics*, **2010**; 77(12): 2385–2402.

[11] Hyde TH, Ali BS and Sun W, Analysis and design of a small, two-bar creep test specimen. *Journal of Engineering Materials and Technology*, **2013**; 135(4): 041006

[12] Hyde TH, Ali BS and Sun W, On the determination of material creep constants using miniature creep test specimens. *Journal of Engineering Materials and Technology*, **2014**; 136(2): 021006.

[13] Hyde TH, Li R, Sun W, et al., A simplified method for predicting the creep crack growth in P91 welds at 650 C. *Proceedings of the Institution of Mechanical Engineers, Part L: Journal of Materials Design and Applications*, **2010**; 224(4): 208–219.

[14] Hyde TH, Saber M and Sun W, Testing and modelling of creep crack growth in compact tension specimens from a P91 weld at 650_C. *Engineering Fracture Mechanics*, **2010**; 77(15): 2946–2957.

[15] Hyde TH, Saber M and Sun W, Creep crack growth data and prediction for a P91 weld at 650_C. International *Journal of Pressure Vessels and Piping*, **2010**; 87(12): 721–729.

[16] Bartsch H, A new creep equation for ferritic and martensitic steels. *Steel Research*, **1995**; 66: 384–388.

[17] Holdsworth SR and Mazza E, Exploring the applicability of the LICON methodology for a 1%CrMoV steel. *Materials at High Temperatures*, **2008**; 25: 267–276.

[18] Y. Xiao, A multi-mechanism damage coupling model, *Int. J. Fatigue* 26 (11) (**2004**) 1241–1250.

[19] R.P. Skelton, D. Gandy, Creep–fatigue damage accumulation and interaction diagram based on metallographic interpretation of mechanisms, *Mater. High Temp*. 25 (1) (**2008**) 27–54.

[20] L. Zhao, L. Xu, K. Nikbin, Predicting failure modes in creep and creep-fatigue crack growth using a random

grain/grain boundary idealized microstructure meshing system, *Mater. Sci. Eng. A* 704 (**2017**) 274–286.

[21] L. Xu, J. Rong, L. Zhao, H. Jing, Y. Han, Creep-fatigue crack growth behavior of G115 steel at 650◦ C, *Mater. Sci. Eng. A* 726 (**2018**) 179–186.

[22] Z. Tang, H. Jing, L. Xu, L. Zhao, Y. Han, B. Xiao, Y. Zhang, H. Li, Investigating crack propagation behavior and damage evolution in G115 steel under combined steady and cyclic loads, *Theor. Appl. Fract. Mech*. 100 (**2019**) 93–104.

[23] Z.C. Fan, X.D. Chen, L. Chen, J.L. Jiang, A CDM-based study of fatigue–creep interaction behavior, *Int. J. Press. Vessel. Pip.* 86 (9) (**2009**) 628–632.

[24] A. Huang, W. Yao, F. Chen, Analysis of fatigue life of PMMA at Different frequencies based on a new damage mechanics model, *Math. Probl. Eng*. (**2014**) 352676.

[25] N. Liu, H. Dai, L. Xu, Z. Tang, C. Li, J. Zhang, J. Lin, Modeling and effect analysis on crack growth behavior of Hastelloy X under high temperature creep-fatigue interaction, *Int. J. Mech. Sci*. 195 (**2021**), 106219.

[26] Kamaludin, S., Thamburaja, P. Efficient Neighbour Search Algorithm for Nonlocal-Based Simulations—Application to Failure Mechanics. *J Fail. Anal. and Preven*. 23, 540–547 (**2023**).

[27] Bazant, Z.P., Belytschko, T.B. and Chang, T. P., Continuum theory for strain-softening, *Journal of the Engineering Mechanics Division, ASCE*, **1984**; vol. 110, No.12: 1666-1692.

[28] Bazant, Z.P. and Pijaudier-Cabot, G., Nonlocal continuum damage, localization instability and convergence, *Journal of Applied Mechanics*, **1988**; Vol. 55, No 2: 287- 293.

[29] Bazant, Z. P. F.ASCE., Nonlocal damage theory based on micromechanics of crack interactions, *Journal of Engineering Mechanics*, March, **1994**; Vol. 120, No. 3: 593-617.

[30] Abu Al-Rub, R. K. and Voyiadjis, G. Z., A direct finite element implementation of the gradient-dependent theory, *International Journal for Numerical Methods in Engineering*, **2005**; 63: 603-629.

[31] Dorgan, R. J. and Voyiadjis, G. Z., A Mixed Finite Element Implementation of a Gradient-enhanced Coupled Damage–Plasticity Model, *International Journal of Damage Mechanics*, **2006**; Vol. 15: 201-235.

[32] Andrade FXC, César De Sá JMA, Andrade Pires FM, A ductile damage nonlocal model of integral-type at finite strains: Formulation and numerical issues. *International Journal of Damage Mechanics*, **2011**; 20: 515–557.

[33] Brunet M, Morestin F, Walter H, Damage identification for anisotropic sheet-metals using a non-local damage model. *International Journal of Damage Mechanics*, **2016**; 13: 35–57.

[34] Jirásek M, Non-local damage mechanics with application to concrete. *Revue Française de Génie Civil*, **2004**; 8: 683–707.

[35] Belytschko T, Gracie R, Ventura G, A review of extended/generalized finite element methods for material modeling. *Modelling and Simulation in Materials Science and Engineering*, **2009**; 17: 43001.

[36] Li X, Chen J, An extended cohesive damage model for simulating arbitrary damage propagation in engineering materials. *Computer Methods in Applied Mechanics and Engineering*, **2017**; 315: 744–759.

[37] Li, Xiaole & Gao, Weicheng & Liu, Wei., A mesh objective continuum damage model for quasi-brittle crack modelling and finite element implementation. *International Journal of Damage Mechanics*, **2019**; vol 28.

[38] Seupel, A., Hütter, G., Kuna, M., An efficient FE-implementation of implicit gradient enhanced damage models to simulate ductile failure, *Engineering Fracture Mechanics*, **2018**.

[39] Alban de Vaucorbeil, Vinh Phu Nguyen, Tushar Kanti Mandal, Mesh objective simulations of large strain ductile fracture: A new nonlocal Johnson-Cook damage formulation for the Total Lagrangian Material Point Method, *Computer Methods in Applied Mechanics and Engineering*, **2022**; Volume 389.

[40] Chow, C. L., Mao, J., & Shen, J., Nonlocal Damage Gradient Model for Fracture Characterization of Aluminum Alloy. *International Journal of Damage Mechanics*, **2011**; 20(7), 1073–1093.

[41] V.B. Pandey, M. Kumar, I.V. Singh, B.K. Mishra, S. Ahmad, A.V. Rao, V. Kumar, Mixed-mode creep crack growth simulations using continuum damage mechanics and virtual node XFEM, in: *Structural Integrity Assessment*, Springer, Singapore, **2020**, pp. 275–284.

[42] V.B. Pandey, S.S. Samant, I.V. Singh, B.K. Mishra, An improved methodology based on continuum damage mechanics and stress triaxiality to capture the constraint effect during fatigue crack propagation, *Int. J. Fatigue* 140 (**2020**), 105823.

[43] V.B. Pandey, I.V. Singh, B.K. Mishra, Complete Creep Life Prediction Using Continuum Damage Mechanics and XFEM, in: *Recent Advances in Computational Mechanics and Simulations*, Springer, Singapore, **2020**, pp. 169-176.

[44] V.B. Pandey, I.V. Singh, B.K. Mishra, S. Ahmad, A.V. Rao, V. Kumar, Creep crack simulations using continuum damage mechanics and extended finite element method, *Int. J. Damage Mech* 28 (1) (**2019**) 3–34.

[45] V.B. Pandey, I.V. Singh, B.K. Mishra, S. Ahmad, A.V. Rao, V. Kumar, A new framework based on continuum damage mechanics and XFEM for high cycle fatigue crack growth simulations, *Eng. Fract. Mech*. 206 (**2019**) 172–200.

[46] V.B. Pandey, I.V. Singh, B.K. Mishra, A Strain-based continuum damage model for low cycle fatigue under different strain ratios, *Eng. Fract. Mech*. 242 (**2021**), 107479.

[47] S.S. Samant, V.B. Pandey, I.V. Singh, R.N. Singh, Effect of double austenitization treatment on fatigue crack growth and high cycle fatigue behavior of modified 9Cr–1Mo steel, *Mater. Sci. Eng. A* Vol. 788,139495 (**2020**).

[48] Ashby MF, A first report on deformation–mechanism maps. *Acta Metallurgica*, **1972**; 20: 887–897.

[49] Maruyama K, In: Abe F, Kern TU and Viswanathan R (eds), Fundamental aspects of creep deformation and deformation mechanism map. Creep–Resistant Steels. Cambridge, England: *Woodhead Publishing and CRC Press*, **2008**; pp. 265–278.

[50] Holdsworth SR and Mazza E, Exploring the applicability of the LICON methodology for a 1%CrMoV steel. *Materials at High Temperatures*, **2008**; 25: 267–276